

**Interfacial electronic and magnetic properties of a  $Y_{0.6}Pr_{0.4}Ba_2Cu_3O_7/La_{2/3}Ca_{1/3}MnO_3$  superlattice**Jian Liu,<sup>1,2,\*</sup> B. J. Kirby,<sup>3</sup> B. Gray,<sup>1</sup> M. Kareev,<sup>1</sup> H.-U. Habermeier,<sup>4</sup> G. Cristiani,<sup>4</sup> J. W. Freeland,<sup>5</sup> and J. Chakhalian<sup>1,†</sup><sup>1</sup>*Department of Physics, University of Arkansas, Fayetteville, Arkansas 72701, USA*<sup>2</sup>*Advanced Light Source, Lawrence Berkeley National Laboratory, Berkeley, California 94720, USA*<sup>3</sup>*Center for Neutron Research, National Institute of Standards and Technology, Gaithersburg, Maryland 20899, USA*<sup>4</sup>*Max Plank Institute for Solid State Research, D-70569 Stuttgart, Germany*<sup>5</sup>*Advanced Photon Source, Argonne National Laboratory, Argonne, Illinois 60439, USA*

(Received 15 June 2011; revised manuscript received 28 August 2011; published 28 September 2011)

Resonant soft x-ray absorption spectroscopy and diffuse neutron scattering were used to study the interfacial properties of  $Y_{0.6}Pr_{0.4}Ba_2Cu_3O_7/La_{2/3}Ca_{1/3}MnO_3$  superlattices. Dramatic changes from the bulk in the spectral line shape, energy position, and linear-polarization dependence of the Cu  $L_3$ -edge reveal a striking interfacial modification. The similarities to the case without Pr substitution confirm the strongly hybridized covalent Cu-O-Mn bond as the underlying driving mechanism. On the other hand, relative differences, including reduced charge transfer and interfacial orbital reconstruction, are observed and attributed to raising of the Fermi level of the cuprate layer with Pr substitution. Neutron reflectometry reveals an oscillatory behavior in the rapidly increasing diffuse scattering with decreasing temperature. Temperature- and field-dependent measurements indicate that the origin is associated with the buckling caused by the structural phase transition of the SrTiO<sub>3</sub> substrate rather than the superconducting or magnetic transition.

DOI: [10.1103/PhysRevB.84.092506](https://doi.org/10.1103/PhysRevB.84.092506)

PACS number(s): 74.78.Fk, 73.20.-r, 75.70.Cn, 74.45.+c

The artificial interfacing of distinct materials has been an intriguing way to explore fascinating phenomena unattainable in the bulk. Recently, great attention has been drawn by heterostructures consisting of correlated oxides due to their diverse ground states, where interactions between competing orderings can be controlled by manipulating the interfacial couplings among the multiple degrees of freedom of correlated electrons.<sup>1-4</sup>

A prominent example is the case of heterostructures created from a high- $T_c$  cuprate and a colossal-magnetoresistance manganite, such as  $YBa_2Cu_3O_7$  (YBCO) and  $La_{2/3}Ca_{1/3}MnO_3$  (LCMO). Due to the incompatibility of  $d$ -wave superconductivity (SC) and ferromagnetism, these two order parameters were found to mutually suppress each other in YBCO/LCMO heterostructures with a large length scale.<sup>5,6</sup> On the other hand, a coupling of the superconducting layers was observed and has been attributed to a long-range proximity effect.<sup>7</sup> Moreover, a surprising inverse spin-switch effect, where parallel alignment of the ferromagnetic LCMO layers enhances the transition temperature of the sandwiched YBCO layer, has been recently found.<sup>8</sup> To account for these unconventional long-range proximity effects, the microscopic exchange interaction<sup>9-11</sup> and orbital reconstruction<sup>12</sup> at the YBCO/LCMO interfaces are believed to be crucial.<sup>13,14</sup>

The microscopic picture of the interfacial couplings in YBCO/LCMO superlattices (SLs) has been shown by previous neutron reflectivity (NR) and x-ray absorption spectroscopy (XAS) studies, where a lateral splitting of the SL Bragg peak below the superconducting transition was observed and a net magnetic moment was induced in the interfacial CuO<sub>2</sub> plane with an intriguing antiferromagnetic coupling to Mn.<sup>9,10,15</sup> This antiparallel alignment was explained by interfacial orbital reconstruction where a significant number of holes occupy the Cu  $d_{3z^2-r^2}$  orbital due to the strong covalent Cu-O-Mn bond.<sup>12</sup> The focus of YBCO/LCMO interface studies has, however, been limited to optimally doped YBCO. In this Brief

Report, we report our study on (Y,Pr)BCO/LCMO SLs using linearly polarized XAS and off-specular NR. We utilize the unique control of Pr substitution on the electronic structure of the  $RBa_2Cu_3O_7$  ( $R$  = rare earth) family; Pr is the only rare earth that maintains the crystal structure throughout the entire doping range and suppresses SC at the same time.<sup>16,17</sup>

SLs with a nominal structure of [(Y,Pr)BCO (100 Å)/LCMO (100 Å)]<sub>5</sub> were grown on atomically flat (001) SrTiO<sub>3</sub> (STO) single-crystal substrates by pulsed laser deposition with a KrF excimer laser (248 nm).<sup>9</sup> The Pr substitution of Y was set to be 40%. Symmetrical scans of x-ray diffraction show all (00 $l$ ) reflections of both (Y,Pr)BCO and LCMO layers without any additional peaks, confirming the single-phase and high-quality  $c$ -axis-oriented epitaxial growth. The corresponding (Y,Pr)BCO  $c$ -axis lattice parameter is around 11.66(3) Å, which is consistent with the reported bulk value of (Y,Pr)BCO.<sup>18</sup>

The temperature-dependent resistance was measured in a physical property measurement system (Quantum Design) with magnetic fields applied perpendicular to the film surface. The result shown in Fig. 1 reveals the well-defined superconducting and magnetic behavior of the SL. At zero field, a sharp superconducting transition  $T_{SC}$  occurs around 50 K, much lower than in the case with optimal doping, indicative of uniform Pr substitution. However, it is slightly higher than that in the bulk with a 40% Pr doping ratio,<sup>18</sup> indicating that the actual Pr concentration is likely lower than the nominal one, probably due to the relatively lower thermodynamic stability of  $PrBa_2Cu_3O_7$ .<sup>19</sup> As a field of 6 T is applied,  $T_{SC}$  is suppressed to around 30 K, and the transition is significantly broadened, accompanied by a positive magnetoresistance arising from vortex motion.<sup>20</sup> Compared to the case where the field was applied in the  $ab$  plane of YBCO/LCMO SLs,<sup>12</sup> the induced suppression and broadening by a field along the  $c$  axis are much more pronounced and characteristic of superconducting cuprates due to the two-dimensional layered structure.<sup>21</sup> At

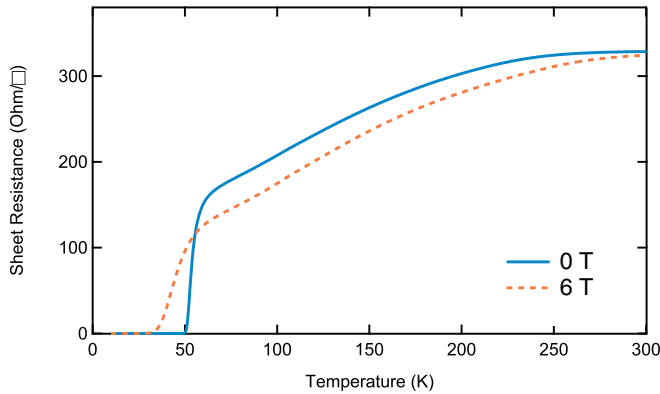


FIG. 1. (Color online) Resistance vs temperature without magnetic field (solid curve) and with a magnetic field (dashed curve) of 6 T perpendicular to the film surface.

higher temperatures, negative magnetoresistance is observed resulting from the ferromagnetic state of LCMO. These characteristic bulklike behaviors further confirm the high-quality growth of both (Y,Pr)BCO and LCMO layers.

To investigate the effect of suppression of SC on the interfacial orbital reconstruction, linearly polarized XAS experiments were performed at the 4-ID-C beamline of the Advanced Photon Source at Argonne National Laboratory.<sup>22</sup> X-rays near the Cu  $L_3$ -edge with polarizations along the  $c$  axis and in the  $ab$  plane were used to obtain x-ray linear dichroism at 30 K. Absorption spectra were recorded simultaneously in both fluorescence yield (FY) mode and total electron yield (TEY) mode.

Figure 2 shows the normalized spectra of the Cu  $L_3$ -edge with in-plane and out-of-plane polarizations. The upper curves correspond to the spectra recorded in the FY mode, which is sensitive to the bulk of the SL. The FY data for both polarizations show a main peak at 930.1 eV, corresponding to the Cu  $2p^63d^9 \rightarrow 2p^53d^{10}$  transition. On the high-energy side of the main peaks, there exists a relatively small shoulder

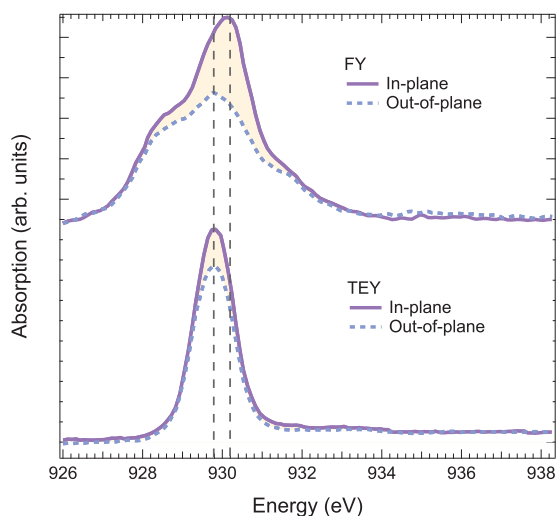


FIG. 2. (Color online) Normalized linearly polarized x-ray absorption spectra at the Cu  $L_3$ -edge taken in (upper curves) bulk-sensitive fluorescence mode and (lower curves) interface-sensitive total electron yield mode. Dashed lines are guides to eyes.

due to the transition to the  $2p^53d^{10}\underline{L}$  final state from the  $2p^63d^9\underline{L}$  initial state, which is strongly hybridized with the  $2p^63d^{10}\underline{L}$  configuration (here  $\underline{L}$  denotes an oxygen ligand hole). This shoulder is the signature of the Zhang-Rice (ZR) singlet state.<sup>23</sup> Such an absorption line shape of the Cu  $L_3$ -edge is typical in superconducting cuprates. Additionally, for both polarizations, there is a broad shoulder at the low-energy side of the main peak due to the Pr  $M_5$ -edge which partially overlaps with the Cu  $L_3$ -edge. The observation and assignment above are consistent with other reported XAS of Pr-doped cuprates.<sup>24–26</sup> In spite of these common features of the FY data for both polarizations, a linear dichroic effect is clearly seen in the upper curves of Fig. 2 with the difference between the two polarizations highlighted in light yellow (gray). This polarization dependence significantly decreases and almost disappears when passing the Pr  $M_5$ -edge from the Cu  $L_3$ -edge. Since, to our best knowledge, no linear dichroism at the Pr  $M$  edge has been reported in the literature for Pr-doped cuprates, based on the observed signal we conclude that linear-polarization dependence is absent at the Pr  $M$  edge. Consequently, by taking the Pr shoulder as the reference, one can see that the absorption of the in-plane polarization is much more intense than that of the out-of-plane polarization, especially at the main peak. This implies that the holes on the Cu  $d$  shell predominantly occupy the planar  $d_{x^2-y^2}$  orbital, which is also observed in all other superconducting cuprates.<sup>27,28</sup>

In contrast, the spectra from the TEY mode, which probes the Cu-O-Mn coupling at the first interface covered by the top LCMO layer,<sup>12</sup> display a dramatically different picture of the electronic structure on the Cu site. As seen in the lower curves of Fig. 2, the Cu  $L_3$ -edge exhibits a line shape distinct from that of the FY mode. In particular, the high-energy shoulder is no longer present, implying that the ZR state is disrupted at the interface. Moreover, the position of the main absorption peak is shifted by  $\sim 0.3$  eV toward lower energy for both polarizations, which is the sign of charge transfer across the interface between two materials with different work functions. Compared to the Cu  $L_3$ -edge positions of other Cu valences, such a chemical shift corresponds to a charge transfer of less than  $0.15e$  per Cu ion.<sup>29</sup> Furthermore, the polarization dependence of the absorption at the interface is much weaker, which is the signature of orbital reconstruction. The strong enhancement of the absorption intensity of the out-of-plane polarization illustrates that a large hole population resides on the  $d_{3z^2-r^2}$  orbital. Note that this sharp contrast between the TEY and FY data shows the strong suppression of the bulklike absorption signal (including both Cu and Pr edges) beyond the interfacial plane in the TEY mode, due to the combination of the very shallow probing depth and the thick LCMO top layer. Consequently, the absorption of the interfacially coupled Cu sites is amplified and dominates the TEY, signifying the striking interfacial reconstructions from the bulk.

These electronic and orbital reconstructions are reminiscent of that at the interface between optimally doped YBCO and LCMO,<sup>12</sup> in spite of the suppressed SC by Pr substitution. This analogy verifies that the interfacial modification from the bulk is driven by the robust Cu-O-Mn covalent bond with strong hybridization. On the other hand, a close comparison

between the two cases reveals significant differences. First of all, the interfacial orbital occupation is more bulklike, evidenced by the relative stronger absorption of the in-plane polarization. Furthermore, the amount of transferred charge is reduced in the present case, shown by the smaller shift of the absorption peak. The smaller charge transfer between the two layers could be attributed to Pr substitution, which is known to push the originally occupied so-called Fehrenbacher-Rice band above the ZR band. This emerging band is caused by the strong hybridization between Pr and O, and depletes the holes from the ZR band, resulting in raising of the Fermi level which originally lies across the ZR band but is now pinned within the Fehrenbacher-Rice band.<sup>16,17,30</sup> Since the orbital reconstruction relies on the hole transfer from the YBCO layer to the LCMO layer through the interfacial Cu-O-Mn antibonding state where the Cu  $d_{3z^2-r^2}$  orbital is strongly mixed,<sup>12</sup> a reduced charge transfer due to a smaller difference in the Fermi level would favor a more bulklike orbital occupation at the interface.

Having obtained the effect of Pr substitution on the interfacial electronic structure, we took advantage of the suppressed  $T_{SC}$  to study the nature of the oscillatory neutron diffuse scattering previously observed for optimally doped YBCO/LCMO SLs.<sup>9</sup> Note that a similar splitting of the SL Bragg peak was observed on a (Y,Pr)BCO/LCMO SL by x-ray scattering and attributed to STO structural phase transitions.<sup>31</sup> Here, by virtue of the sensitivity of NR to both the structural and magnetic composition of multilayer films,<sup>32,33</sup> we performed temperature- and field-dependent measurements with polarized neutrons at the NIST Center for Neutron Research, using the AND/R and NG-1 reflectometers.<sup>34,35</sup> For all measurements, the sample was mounted using a flexible aluminum backing (to minimize stress) and was cooled from room temperature to 150 K in zero field and then further cooled to 7 K in the presence of an applied magnetic field.

Figure 3 shows unpolarized neutron scattering reciprocal space maps measured by a position-sensitive detector. Scattering along the  $z$  component of wave vector transfer ( $Q_z$ ) (specular scattering) originates from depth-dependent structural and magnetic features, while scattering along the  $Q_x$  axis (diffuse scattering) corresponds to planar features. At room temperature [Fig. 3(a)], purely nuclear scattering is observed along the specular ridge ( $Q_x = 0$ ) and a SL Bragg peak is clearly observable ( $Q_z \approx 0.035 \text{ \AA}^{-1}$ ), confirming the coherent growth and well-controlled superperiod of the SL.

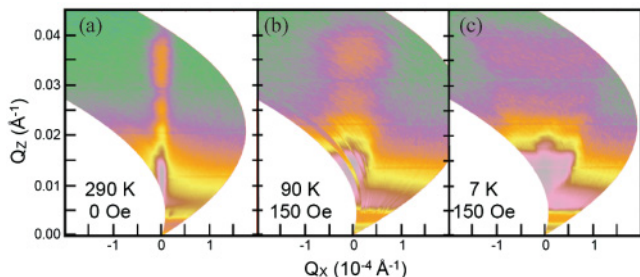


FIG. 3. (Color online) Off-specular neutron reflectivity taken at room temperature, 90 K, and 7 K with a 15 mT cooling field applied parallel to the layers and perpendicular to the beam.

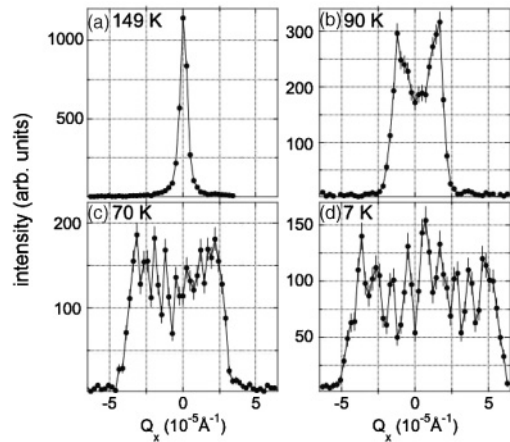


FIG. 4. Temperature-dependent unpolarized neutron transverse scans at  $Q_z = 0.0139 \text{ \AA}^{-1}$  (right below the critical edge). Error bars correspond to  $\pm\sigma$ . Lines are guides to the eye.

As the temperature is reduced, the specular ridge measured at 90 K and 7 K [Figs. 3(b) and 3(c)] dramatically diffuses along the  $Q_x$  direction, indicating significantly increased in-plane inhomogeneity. To further investigate this planar inhomogeneity, a series of high-resolution “transverse scans” (fixed  $Q_z$ ) were taken using a  $^3\text{He}$  point detector. Figure 4 shows temperature-dependent, unpolarized beam transverse scans taken at  $Q_z = 0.0139 \text{ \AA}^{-1}$  (just below the critical edge) in a 650 mT field. At low temperatures, diffuse scattering is again observed, but in this case pronounced oscillations in  $Q_x$  are clearly resolvable. Qualitatively similar results were obtained at a 15 mT field (not shown). Notably, this oscillatory diffuse scattering is present both above and below  $T_{SC}$ , indicating that the onset of SC plays no role in its origin. To examine the role of the magnetic phase transition in this scattering, polarized beam transverse scans were taken at the first SL Bragg peak after cooling in 650 and 15 mT, respectively. As can be seen in Fig. 5, non-spin-flip scattering of spin-up or spin-down

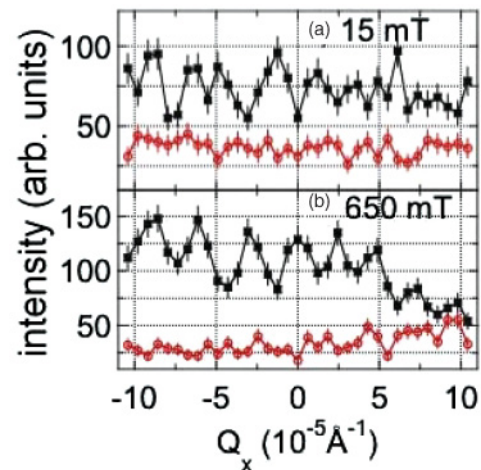


FIG. 5. (Color online) Field-dependent non-spin-flip scattering of polarized neutron transverse scans at  $Q_z = 0.035 \text{ \AA}^{-1}$  with spin-up (solid square) and spin-down (open circle) neutrons. Error bars correspond to  $\pm\sigma$ . Lines are guides to the eye.



neutrons is evident (no significant spin-flip scattering could be detected). While the overall spin splitting (related to the total sample magnetization<sup>32,33</sup>) increases with increasing field, the oscillatory behaviors of the diffuse scattering are similar for both fields, strongly suggesting that it is not a magnetic effect. Instead, it is exceedingly likely that the observed in-plane modulation described above is primarily due to the STO structural phase transition ( $T_{\text{STO}} = 105$  K) which is associated with crystallographic twinning and surface buckling.<sup>9,36</sup> Specifically, we expect that the SL film becomes faceted below  $T_{\text{STO}}$ , causing the specular reflection to split into multiple reflections, similarly to the observation by x-ray scattering.<sup>31</sup>

In conclusion, we have observed electronic and orbital reconstructions at the interface of high-quality (Y,Pr)BCO/LCMO SLs by linearly polarized XAS at the Cu  $L_3$ -edge. The highly covalent Cu-O-Mn bond responsible for

the reconstructions was found to be vigorous, despite the suppressed SC compared with YBCO/LCMO SLs. However, since Pr substitution raises the Fermi level by pushing out the Fehrenbacher-Rice band which depletes holes in the ZR band, reduced interlayer charge transfer was observed, along with a reduction of the orbital reconstruction at the interface. NR data revealed temperature-dependent oscillatory diffuse scattering, indicative of a significant in-plane modulation of the SL, which can be attributed to buckling of the film due to the structural phase transition of the STO substrate.

J. C. was supported by DOD-ARO under Contract No. 0402-17291 and NSF Contract No. DMR-0747808. Work at the Advanced Photon Source, Argonne is supported by the US Department of Energy, Office of Science under Contract No. DEAC02-06CH11357.

\*jxl026@uark.edu

<sup>†</sup>jchakhal@uark.edu

<sup>1</sup>A. Ohtomo and H. Y. Hwang, *Nature (London)* **427**, 423 (2004).

<sup>2</sup>J. Garcia-Barriocanal *et al.*, *Nature Commun.* **1**, 82 (2010).

<sup>3</sup>S. S. A. Seo *et al.*, *Phys. Rev. Lett.* **104**, 036401 (2010).

<sup>4</sup>J. Liu, S. Okamoto, M. van Veenendaal, M. Kareev, B. Gray, P. Ryan, J. W. Freeland, and J. Chakhalian, *Phys. Rev. B* **83**, 161102(R) (2011).

<sup>5</sup>Z. Sefrioui, D. Arias, V. Pena, J. E. Villegas, M. Varela, P. Prieto, C. Leon, J. L. Martinez, and J. Santamaria, *Phys. Rev. B* **67**, 214511 (2003).

<sup>6</sup>T. Holden *et al.*, *Phys. Rev. B* **69**, 064505 (2004).

<sup>7</sup>V. Pena, Z. Sefrioui, D. Arias, C. Leon, J. Santamaria, M. Varela, S. J. Pennycook, and J. L. Martinez, *Phys. Rev. B* **69**, 224502 (2004).

<sup>8</sup>N. M. Nemes *et al.*, *Phys. Rev. B* **78**, 094515 (2008).

<sup>9</sup>J. Chakhalian *et al.*, *Nature Phys.* **2**, 244 (2006).

<sup>10</sup>J. Stahn *et al.*, *Phys. Rev. B* **71**, 140509 (2005).

<sup>11</sup>J. W. Freeland *et al.*, *Appl. Phys. Lett.* **90**, 242502 (2007).

<sup>12</sup>J. Chakhalian *et al.*, *Science* **318**, 1114 (2007).

<sup>13</sup>J. Salafranca and S. Okamoto, *Phys. Rev. Lett.* **105**, 256804 (2010).

<sup>14</sup>X. Yang *et al.*, e-print arXiv:0911.4349.

<sup>15</sup>R. Werner *et al.*, *Phys. Rev. B* **82**, 224509 (2010).

<sup>16</sup>A. I. Liechtenstein and I. I. Mazin, *Phys. Rev. Lett.* **74**, 1000 (1995); R. Fehrenbacher and T. M. Rice, *ibid.* **70**, 3471 (1993).

<sup>17</sup>I. I. Mazin and A. I. Liechtenstein, *Phys. Rev. B* **57**, 150 (1998).

<sup>18</sup>J. L. Peng, P. Klavins, R. N. Shelton, H. B. Radousky, P. A. Hahn, and L. Bernardez, *Phys. Rev. B* **40**, 4517 (1989).

<sup>19</sup>A. Kebede *et al.*, *Phys. Rev. B* **40**, 4453 (1989).

<sup>20</sup>T. T. M. Palstra, B. Batlogg, L. F. Schneemeyer, and J. V. Waszczak, *Phys. Rev. Lett.* **61**, 1662 (1988).

<sup>21</sup>For example, M. Oda, Y. Hidaka, M. Suzuki, and T. Murakami, *Phys. Rev. B* **38**, 252 (1988).

<sup>22</sup>J. W. Freeland *et al.*, *Rev. Sci. Instrum.* **73**, 1408 (2001).

<sup>23</sup>F. C. Zhang and T. M. Rice, *Phys. Rev. B* **37**, 3759 (1988).

<sup>24</sup>U. Neukirch *et al.*, *Europhys. Lett.* **5**, 567 (1988).

<sup>25</sup>J. M. Chen *et al.*, *Chem. Phys. Lett.* **294**, 209 (1998).

<sup>26</sup>J. M. Chen, R. S. Liu, J. G. Lin, C. Y. Huang, and J. C. Ho, *Phys. Rev. B* **55**, 14586 (1997).

<sup>27</sup>N. Nucker, E. Pellegrin, P. Schweiss, J. Fink, S. L. Molodtsov, C. T. Simmons, G. Kaindl, W. Frentrup, A. Erb, and G. Muller-Vogt, *Phys. Rev. B* **51**, 8529 (1995).

<sup>28</sup>C. T. Chen *et al.*, *Phys. Rev. Lett.* **66**, 104 (1991).

<sup>29</sup>F. M. F. de Groot, *J. Electron Spectrosc. Relat. Phenom.* **67**, 529 (1994).

<sup>30</sup>M. Merz *et al.*, *Phys. Rev. B* **55**, 9160 (1997).

<sup>31</sup>J. Hoppler, J. Stahn, H. Bouyanfif, V. K. Malik, B. D. Patterson, P. R. Willmott, G. Cristiani, H. U. Habermeier, and C. Bernhard, *Phys. Rev. B* **78**, 134111 (2008).

<sup>32</sup>C. F. Majkrzak, K. V. O'Donovan, and N. F. Berk, in *Neutron Scattering From Magnetic Materials*, edited by T. K. Chatterji (Elsevier Science, Amsterdam, 2005).

<sup>33</sup>Hartmut Zabel, Katharina Theis-Bröhl, and Boris P. Toperverg, in *Handbook of Magnetism and Advanced Magnetic Materials*, edited by Helmut Kronmüller and Stuart Parkin, Vol. 3 (Wiley, New York, 2007).

<sup>34</sup>J. A. Dura *et al.*, *Rev. Sci. Instrum.* **77**, 074301 (2006).

<sup>35</sup>See [<http://www.ncnr.nist.gov/instruments/andr>] and [<http://www.ncnr.nist.gov/instruments/ng1refl>].

<sup>36</sup>V. K. Vlasko-Vlasov, Y. K. Lin, D. J. Miller, U. Welp, G. W. Crabtree, and V. I. Nikitenko, *Phys. Rev. Lett.* **84**, 2239 (2000).